沙漠研究 **22**-1, 291 -294 (2012)
Journal of Arid Land Studies

"ICAL 1 / DT X"
－Refereed Paper－

Detecting Soil Characteristics in Arid Land by Using Landsat ETM+: Case Study of Beni-Swif, Egypt

Kunihiko YOSHINO*[1)], Khishigsuren NYAMSAMBUU[2)], Yudi SETIAWAN[2)] and Abeer ELWAN[2)]

Abstract: Remote sensing can discriminate deposits of target minerals. The objectives of this research are to characterize minerals in the soil of Beni-Swif area in Egypt and to map the distribution of soil classes based on their mineral contents estimated from Landsat ETM+ data. Eight typical minerals were identified based on spectral reflectance database in the module of ERDAS Imagine software for Landsat ETM+ images. Eight minerals were identified according to the visual analysis; they are: Albite, Calcite, Dolomite, Gypsum, Halloysite, Kaolinite, Muscovite and Montmorillonite. According to the contents of each mineral estimated from the soil surface reflectance of the Landsat ETM+ image, seventeen soil classes were classified and their distributions were mapped. The accuracy of the map was validated with 45 soil samples in the study site. This research shows remote sensing is effective to characterize soil in the arid and semi arid regions.

Key Words: Landsat ETM+, Minerals, Soil characteristics, Soil spectral reflectance

1. Introduction

Mineral composition of the soil surface mainly affects on soil behavior because it consists about 97% of the soil volume in the arid regions (Schulze, 2002). Moreover, Kruse *et al*. (1990) suggested that many minerals could be identified and characterized based on their reflected-light spectral characteristics. Their types and concentrations determine important properties such as texture and cation exchange capacity. These properties may in turn have significant effects on many other soil properties such as nutrient availability for plant uptake, available potassium which depends on its released amount from the weathering primary minerals.

Many image processing techniques are used to extract ground surface information such as soil mineral composition from remote sensing spectral data. Information on mineral composition of soils can be derived from their spectral reflectance (Kruse *et al*., 1990). Datasets of soil spectral reflectance have been successfully used for prediction of numerous soil properties (Taylor *et al*., 2002; Gregory *et al*., 2006; Chun-Yu *et al*., 2009). Soil maps are very helpful for better agricultural land management in arid lands. Therefore, the objectives of this research are 1) to characterize minerals in the soil of Beni-Swif area in Egypt and 2) to map the distribution of soil classes based on their mineral contents estimated from Landsat ETM+ data.

2. Methods

2.1. Study area

The study area is located in the arid region in the middle of Egypt (**Fig. 1**). It is characterized by complexly folded and faulted Cretaceous, Pleistocene and Eocene age rocks that host a wide verity of mineral deposits (Ghorab *et al*., 1970). The study area includes two main soil formations; one is the alluvial flood plain and another is westerns desert deposits. Since they have been formed in various geological ages, their mineral compositions are different among those soil properties.

2.2. Measurement of spectral reflectance of soil samples

In order to characterize minerals in the soil of Beni-Swif area in Egypt from spectral reflectance of soil, some topographic and geological maps were analyzed with the field work. Then, forty five soil samples were collected in the study site. After that, they were air-dried, ground gently, and then sieved through a 2 mm sieve. Figure 1 shows the study area and the locations of soil samples.

The spectral reflectance of these sieved soil samples were measured with Shimadzu UV-3600 spectro-photometer and UVProbe software. The measuring wavelength ranged from 220nm to 2600 nm. A white plate of $BaSO_4$ was used as a reflectance standard. The reflectance was measured every 1.0 nm, so each soil sample had totally 2380 data points. These reflectance data were clustered by using the Matlab R2010 software, and classified into some groups of soil. Specific mineral components were detected by comparing absorption

* Corresponding Author: sky@sk.tsukuba.ac.jp
1-1-1 Ten-noudai, Tsukuba, Ibaraki 305-8573
1) Faculty of Engineering, Information and Systems, University of Tsukuba 2) Graduate school of life and environmental sciences, University of Tsukuba

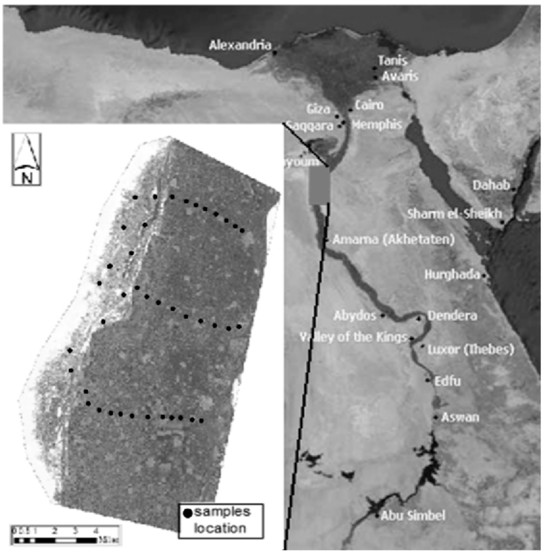

Fig. 1. The study area (Beni-Swif) and soil sample points.

wavelengths in the minerals reflectance library (Clark *et al*., 2003).

As the results of in-situ experiments, differences of the spectral reflectance curves were clearly found between soil samples depending on soil classes. Consequently, types of soil in the study site could be discriminated by using difference of spectral reflectance of soil surface.

2.2. Spectral information derived from satellite remote sensing imagery

In order to map the distribution of soil classes based on their mineral contents estimated from satellite remote sensing data., one Landsat 7 ETM+ image (path/row: 177/40) acquired on May 3, 2003 was analyzed. The image was geometrically corrected and coordinate system was geographic coordinate systems on datum World Geodetic System of 1984 (WGS-84). Then, an atmospheric correction was done using the COST method (Chavez, 1996), which considers a specific bias, gain value, solar angle, minimum and maximum value of each band. As a result, an atmospherically standardized image was obtained.

The spectral analysis was performed using ERDAS IMAGINE 2010 with the spectral library data. The target detection module and orthogonal subspace projection (OSP) method was applied for mapping mineral distribution. The OSP algorithm attempts to eliminate all unwanted or undesired spectral signatures within a pixel. Then, a matched filter algorithm was used to extract the desired spectral signature which exists in that pixel (Harsanyi and Chang, 1994). In this study, this algorithm was applied to assess the contents of target minerals in pixels. Then, a map of the distribution of soil classes based on their mineral contents estimated from Landsat ETM+ data was generated. Finally, using 45 soil

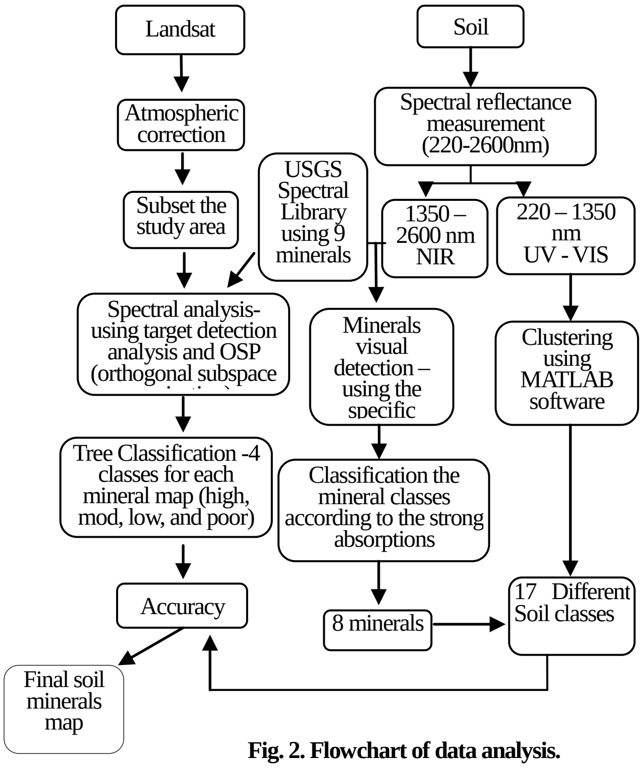

Fig. 2. Flowchart of data analysis.

samples, the accuracy of the map was validated (Fig. 1).

2.3. Procedure of data analysis

Data analysis in this study includes several steps following in-situ experiments, mineral spectral analysis, identification of typical minerals in the study site, estimate minerals' contents and soil class mapping (**Fig. 2**).

3. Results and Discussions

3.1. Soil classification with spectral reflectance

Measured spectral reflectance of soil samples in the study site were classified into seventeen soil classes by clustering. Each soil class shows significantly different characteristics such as soil color and texture (sandy or clayey). Soil in the desert area has coarse texture and light color. Soil in the Nile valley has finer texture and dark color. So, these seventeen soil classes, which correspond to soil groups, have different physical and chemical characteristics, and mineral contents. Eight soil minerals were identified from soil samples according to the visual analysis. They are Albite, Calcite, Dolomite, Gypsum, Halloysite, Kaolinite, Muscovite and Montmorillonite.

As suggested by Clark (1999) and Hunt (1997), soil classes in the study site can be discriminated using Landsat ETM+ image, information of mineral contents in the soil can be obtained, because each mineral has specific absorption wavelength. After conducting OSP method to Landsat

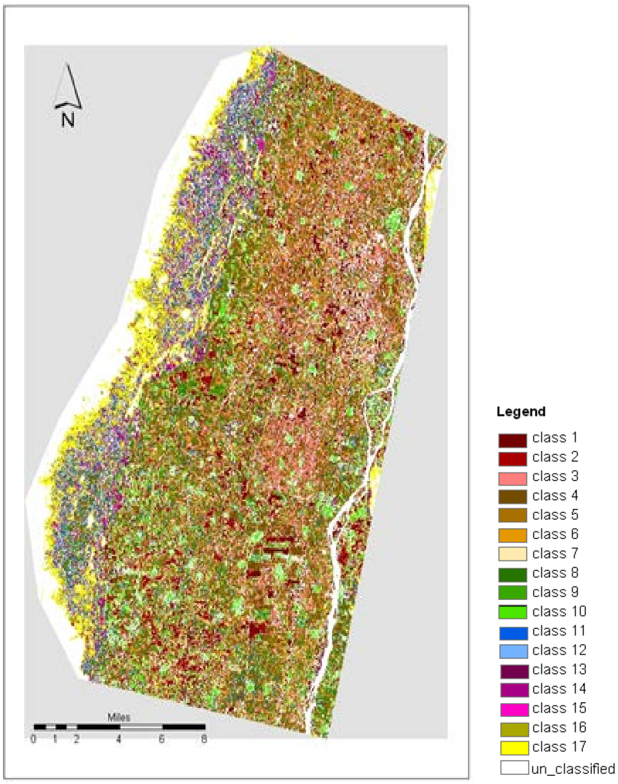

Fig. 3. Soil class map based on mineral content.

Table 1. Mineral content s in each soil class

Class of soil class	Mineral contents
Class 1	Kaolinite (high), dolomite (poor), gypsum, muscovite (mod)
Class 2	Kaolinite (high), albite, calcite (low)
Class 3	Gypsum (poor), kaolinite (mod), hallosite (mod)
Class 4	Kaolinite (high), gypsum (poor)
Class 5	Montmorilonite (high), muscovite (high), albite (high)
Class 6	Hallosite (high), kaolinite (high), albite (high)
Class 7	Hallosite (high), albite (high)
Class 8	Albite (mod), kaolinite (mod)
Class 9	Kaolinite (high), gypsum (poor)
Class 10	Kaolinite (high), muscovite (high), montmorilonit (high), albite (high)
Class 11	Muscovite (mod), gypsum (poor)
Class 12	Albite (high), gypsum (high), muscovite (high)
Class 13	Gypsum (high), hallosite (poor)
Class 14	Kaolinite (low), Albite, calcite (mod)
Class 15	Gypsum (high), calcite (mod)
Class 16	Kaolinite (low), montmorilonit (poor)
Class 17	Gypsum (high), albite, calcite (mod)

ETM+ data, eight maps of each mineral content were developed according to the level of contents of target minerals; high content (more than 75%), moderate content (50% to 75%), low content (25%-50%) and poor content (less than 25%).

Finally, according to the contents of each mineral estimated from the soil reflectance, seventeen soil classes were classified.

3.2. Mapping of soil classes

Based on the above-mentioned results, a soil mineral map was generated (**Fig. 3**). The map shows that the clay minerals (Halloysite, Kaolinite, Muscovite, Montmorillonite) are considerably concentrated in the alluvial plain, and the primary minerals (Albite, Calcite, Dolomite, Gypsum) are quite concentrated in the fringes of desert. Detailed information of mineral contents in each soil class is given in **Table 1**.

The accuracy of the mineral maps was assessed using the 40 soil samples in the study site. The overall accuracy of the (Albite, Calcite, Dolomite, Gypsum, Hallosite, Kaolinite, Muscovite, Montmorillonite) were 51.11%, 73.33%, 71.11%, 15.56%, 68.89%, 71.11%, 48.89%, and 68.89%, respectively. And, kappa-statistics for these minerals were 0.29, 0.60, 0.57, 0.03, 0.53, 0.53, 0.21, 0.43, respectively. These classification accuracies might be insufficient, but the estimated contents of minerals potentially indicate soil characteristics regarding to mineral composition.

Many spots of greenish color (Class 10, 11 and 12) are found in this map. These are spots where Muscovite is highly concentrated. As one of essential elements of Muscovite is potassium, which is rich in the fertilizer for agriculture, these spots might be agricultural lands near villages. According to the local knowledge of this region, locations of these spots are corresponding to villages.

These results show that Landsat ETM+ with a spatial resolution of 30 m is useful for mapping soil characteristics, especially in arid lands, because vegetation covers are less than other climatic regions. These kinds of maps of soil characteristics are very useful for agricultural land planning and land use management in wide areas.

4. Conclusion

Minerals in soil could be recognized using the spectral reflectance in the effective spectral range of 1.0 μm to 2.5 μm. As a result of in-situ experiment, eight minerals were identified in the soil samples in the study site. They are Albite, Calcite, Dolomite, Gypsum, Hallosite, Kaolinite, Muscovite, and Montmorillonite.

Furthermore, a soil map was generated in taking into account mineral composition in soil surface by using Landsat ETM+ in this study. The results of accuracy assessment of this map indicate that additional ground surveys are needed to evaluate accurately. However, some soil characteristic such as uptake nutrient availability, potassium, Cation Exchange

Capacity, ventilation, permeability, bulk density, wind erosion impact and the water saturation could be estimated from soil mineral maps in the further studies. Considering meteorological, social and economical data, soil maps are useful tools for the land evaluation, land management and land resource planning.

Acknowledgment

Authors thank to Mrs. Abeer Elwan for her cooperation to this research work while she was a research student at the University of Tsukuba in 2009-2010.

References

Chavez P.S. Jr. (1996): Image-based atmospheric correction-Revisited and Improved. *Photogrametric Engineering and Remote Sensing*, **62**(9): 1025-1036.

Clark R.N., (1999): *Spectroscopy of Rocks and Minerals, and Principles of Spectroscopy in Manual of Remote Sensing* - Geoscience, Ed. A. Rencz, John Wiley & Sons, New York.

Clark R.N., Swayze G.A., Wise R., Livo K.E., Hoefen, T.M., Kokaly, R.F., Sutley S.J. (2003): USGS Digital Spectral Library splib05a. *USGS Open File Report*. 03: 395.

Congalton R. (1991): A Review of Assessing the Accuracy of Classifications of Remotely Sensed Data. *Remote Sensing of Environment*, **37**: 35-46.

Gregory W., Mc Catry., James B. Reeves (2006): Comparison of near infrared and mid infrared diffuse reflectance spectroscopy for field scale measurement of soil fertility parameters. *Soil science*, **2**(171): 94-102.

Ghorab, M.A., Gezeery, N., Abdin, S. (1970): Studies on the sedimentary basins of Egypt based on recent exploration activities. *Proceeding of the 8th Annual Meeting, Geological Society of Egypt*: 4-6.

Harsanyi J.C, Chang C.I (1994): Hyperspectral image classification and dimensionality reduction: An orthogonal subspace projection approach. *IEEE Transactions on Geoscience and Remote Sensing*, **32**: 779-785.

Hunt G.R. (1980): *Electromagnetic Radiation: The Communication Link in Remote Sensing*. *In* Siegal B.S. and Gillespie A.R eds., Remote Sensing in Geology, John Wiley, New York: 5-45.

Kruse F.A., Lefkoft A.B., Dietz J.B. (1990): *Expert system based mineral mapping using AVIRIS*. University of Coloroda.

Schulze D.G. (2002): *An introduction to soil mineralogy. Soil Mineralogy with Environmental Applications*. Soil Science Society of America, Madison, Wisconsin: 1-34.

Taylor G.R., Dehaan R.L. (2002): Field-derived spectra of salinized soils and vegetation as indicators of irrigation-induced soil salinization. *Remote Sensing of Environment*, **80**: 406-417.

Wu Chun-Yu, Astrid R. Jacobson, Magdeline Laba., Bojeong Kim, Phillippe C.B. (2010): Surrogate Correlations and Near-Infrared Diffuse Reflectance Sensing of Trace Metal Content in Soils. *Water Air Soil Pollution*, **209**(1-4): 377-390.